

TRANSLATIONAL RESEARCH PAPER

Autophagy deficiency in myeloid cells increases susceptibility to obesity-induced diabetes and experimental colitis

Hae-Youn Lee^{a,†}, Jinyoung Kim^{b,c,†}, Wenying Quan^{a,†}, June-Chul Lee^a, Min-Soo Kim^d, Seok-Hyung Kim^e, Jin-Woo Bae^d, Kyu Yeon Hur^a, and Myung-Shik Lee^b

^aDepartments of Medicine, Samsung Medical Center, Sungkyunkwan University School of Medicine, Seoul, Korea; ^bSeverance Biomedical Science Institute and Department of Internal Medicine, Yonsei University College of Medicine, Seoul, Korea; ^cDepartment of Health Sciences and Technology, SAIHST, Sungkyunkwan University School of Medicine, Seoul, Korea; ^dDepartment of Life & Nanopharmaceutical Sciences and Department of Biology, Kyung Hee University, Seoul, Korea; ^eDepartment of Pathology, Samsung Medical Center, Sungkyunkwan University School of Medicine, Seoul, Korea

ABSTRACT

Autophagy, which is critical for the proper turnover of organelles such as endoplasmic reticulum and mitochondria, affects diverse aspects of metabolism, and its dysregulation has been incriminated in various metabolic disorders. However, the role of autophagy of myeloid cells in adipose tissue inflammation and type 2 diabetes has not been addressed. We produced mice with myeloid cell-specific deletion of *Atg7* (autophagy-related 7), an essential autophagy gene (*Atg7* conditional knockout [cKO] mice). While *Atg7* cKO mice were metabolically indistinguishable from control mice, they developed diabetes when bred to *ob/w* mice (*Atg7* cKO-*ob/ob* mice), accompanied by increases in the crown-like structure, inflammatory cytokine expression and inflammasome activation in adipose tissue. M ϕ s (macrophages) from *Atg7* cKO mice showed significantly higher interleukin 1 β release and inflammasome activation in response to a palmitic acid plus lipopolysaccharide combination. Moreover, a decrease in the NAD⁺:NADH ratio and increase in intracellular ROS content after treatment with palmitic acid in combination with lipopolysaccharide were more pronounced in M ϕ s from *Atg7* cKO mice, suggesting that mitochondrial dysfunction in autophagy-deficient M ϕ s leads to an increase in lipid-induced inflammasome and metabolic deterioration in *Atg7* cKO-*ob/ob* mice. *Atg7* cKO mice were more susceptible to experimental colitis, accompanied by increased colonic cytokine expression, T helper 1 skewing and systemic bacterial invasion. These results suggest that autophagy of M ϕ s is important for the control of inflammasome activation in response to metabolic or extrinsic stress, and autophagy deficiency in M ϕ s may contribute to the progression of metabolic syndrome associated with lipid injury and colitis.

ARTICLE HISTORY

Received 29 April 2015
Revised 21 April 2016
Accepted 26 April 2016

KEYWORDS

autophagy; colitis; diabetes; inflammasome; macrophages; obesity

Introduction

Macroautophagy (referred to as autophagy hereafter) is a catabolic cellular process leading to the degradation of the cell's own components inside autolysosomes which are formed by fusion of double-membrane autophagosomes enclosing cellular content to lysosomes. Autophagy plays a critical role in the metabolic adaptation in nutrient deficiency and also in the turnover of dysfunctional or damaged proteins and organelles.¹ Since ER (endoplasmic reticulum) and mitochondria that critically affect β -cell function, insulin release and insulin sensitivity depend on autophagy for proper function,^{2–4} autophagy of several metabolic organs or systemic autophagy affects nutrient metabolism.^{5,6} Furthermore, disturbance of local or systemic autophagy appears to play a role in dysregulated metabolism and in the development of metabolic syndrome or T2D (type 2 diabetes).

Insulin resistance is a prerequisite for the development of T2D and is caused by several factors such as lipid, ROS


(reactive oxygen species), and ER stress.⁷ Besides such well-recognized factors, low-grade inflammation has recently been implicated as an important contributing factor to insulin resistance.⁷ There have been numerous reports showing the role of diverse innate immune receptors in inflammation associated with metabolic syndrome; however, recent papers have presented convincing data suggesting a crucial role of NLRP3 (NLR family, pyrin domain containing 3) inflammasome in this process.^{8–10} The involvement of inflammasome activation in insulin resistance also suggests a potential role of autophagy in the development of insulin resistance, since autophagy is a well-known modulator of inflammasome activation. Thus, autophagy regulates inflammasome activation by participating in the quality control of dysfunctional mitochondria that can augment inflammasome activation and also by removing the inflammasome complex.^{11,12}

As these results suggest that autophagy deficiency is a proinflammatory condition particularly in relation to inflammasome

CONTACT Myung-Shik Lee  mslee0923@yuhs.ac  50 Yonsei-ro Seodaemun-gu, Yonsei University College of Medicine, Seoul 03722, Korea.

Color versions of one or more of the figures in this article can be found online at www.tandfonline.com/kaup.

[†]These authors equally contributed to this work.

 Supplemental data for this article can be accessed on the publisher's website.

activation, deficient autophagy can be a factor in the development of T2D associated with low-grade inflammation and inflammasome activation. Although the role of autophagy of diverse tissues in body metabolism has been intensively investigated,¹³⁻²¹ the importance of autophagy of myeloid cells such as *Mφs* (macrophages) in the regulation of systemic insulin sensitivity and in the development of T2D has not been clearly elucidated. Besides metabolic syndrome, IBD (inflammatory bowel disease) is a prototypic disease associated with autophagy deficiency inducing aggravated tissue inflammation.²² Furthermore, the incidence of IBD is increased by a western diet underscoring the importance of both genetic and environmental factors in the development of IBD.²³ To investigate the role of myeloid cell autophagy in tissue inflammation associated with metabolic syndrome, we generated mice with myeloid cell-specific autophagy deficiency and studied the development of diabetes and metabolic syndrome before and after imposing metabolic stress. We also examined the relationship between myeloid autophagy and the development of experimental colitis using mice with myeloid cell-specific autophagy deficiency.

Results

Metabolic profile of myeloid cell-specific autophagy-deficient mice

We bred *Atg7* cWT (conditional wild-type; *Atg7^{F/F}*) mice with *Lys-Cre* mice where Cre recombinase is under control of the *Lyz2/LysM* (lysozyme 2) promoter to generate mice with myeloid cell-specific deletion of *Atg7* (*Atg7^{F/F}; Lyz2-Cre⁺* mice, described as *Atg7* conditional knockout (*Atg7* cKO) henceforth in the manuscript) (Table S1). PCR analysis validated deletion of floxed segment in genomic DNA from peritoneal *Mφs* of *Atg7* cKO mice (Fig. 1A). Myeloid cell-specific autophagy

deficiency was confirmed by negligible expression of ATG7 protein and accumulation of SQSTM1 (sequestosome 1)/p62, a well-known receptor and substrate of autophagy in peritoneal *Mφs* from *Atg7* cKO mice (Fig. 1B). *Atg7* mRNA expression was also markedly lower in peritoneal *Mφs* from *Atg7* cKO mice (Fig. 1C). Conversion of MAP1LC3A/B (microtubule-associated protein 1 light chain 3, α/β)-I to MAP1LC3A/B-II was defective in *Mφs* from *Atg7* cKO mice that were cultured in serum-free condition to induce autophagy (Fig. 1B).

Apparently, *Atg7* cKO mice were indistinguishable from *Atg7* cWT mice. Metabolically, both male and female *Atg7* cKO mice were not different from *Atg7* cWT mice, as evidenced by normal nonfasting blood glucose levels, body weight, IPGTT (intraperitoneal glucose tolerance test) and ITT (insulin tolerance test) results ($P > 0.1$ for all comparisons) (Fig. 1D to F, Fig. S1, S2 A to C). Since autophagy deficiency is a proinflammatory condition associated with an increased susceptibility to inflammasome activation¹² and inflammasome activation owing to the metabolic stress of lipid injury is implicated in the low-grade tissue inflammation inducing insulin resistance,¹⁰ we imposed metabolic stress to *Atg7* cKO mice by breeding to *ob/w* (heterozygous *Lep* knockout) mice to derive *Atg7* cKO-*ob/ob* mice (Table S1). While male *Atg7* cWT-*ob/ob* mice showed only hyperglycemia, blood glucose levels of male *Atg7* cKO-*ob/ob* mice were significantly higher than those of male *Atg7* cWT-*ob/ob* mice and reached diabetic range ($P < 0.05$ to 0.001) (Fig. 1D). Body weight of male *Atg7* cKO-*ob/ob* mice was not different from that of male *Atg7* cWT-*ob/ob* mice ($P > 0.1$) (Fig. S1). IPGTT showed further impaired glucose intolerance of male *Atg7* cKO-*ob/ob* mice accompanied by an increased AUC (area under the curve) compared to male *Atg7* cWT-*ob/ob* mice ($P < 0.05$ to 0.01) (Fig. 1E). ITT also showed further decreased insulin sensitivity of male *Atg7* cKO-*ob/ob* mice accompanied by a decreased AUC compared to male *Atg7* cWT-*ob/ob* mice ($P < 0.01$ to

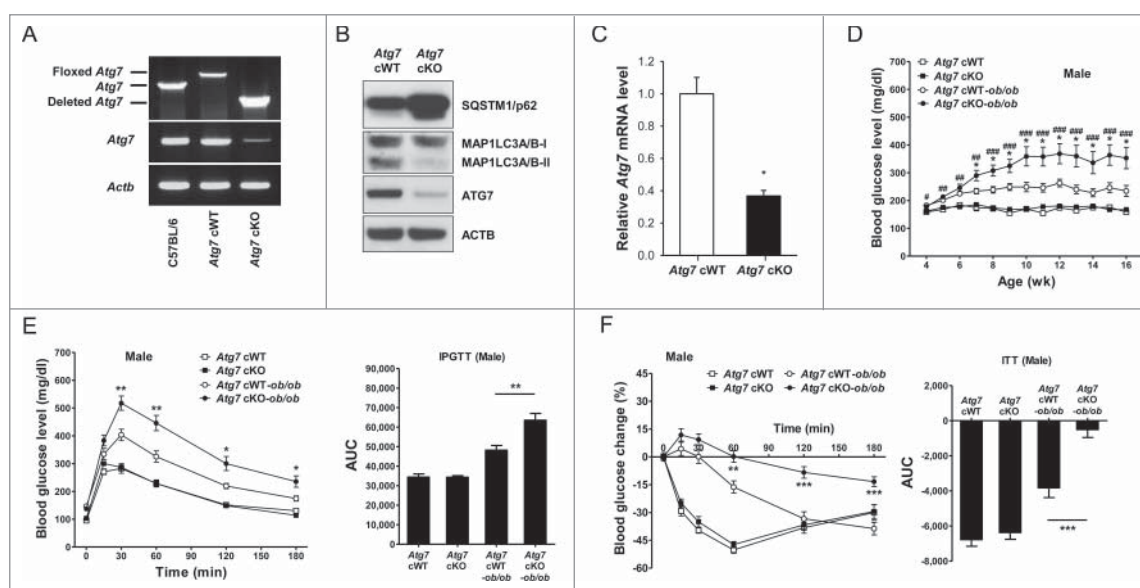


Figure 1. Metabolic profile of male *Atg7* cKO mice. (A) PCR using DNA from peritoneal *Mφs* and primers specific for *Atg7*. (B) Peritoneal *Mφs* were cultured in serum-free conditions for 6 h to induce autophagy, and cell extracts were subjected to western blot analysis. (C) Quantitative RT-PCR was done using mRNA from *Mφs* and specific primers. (D) Nonfasting blood glucose level was determined in male *Atg7* cKO, *Atg7* cKO-*ob/ob* and respective control mice ($n = 10$ to 15). (E) IPGTT was conducted in overnight-fasted 16-wk-old male mice as described in Materials and Methods, and AUC calculated ($n = 5$ to 8). (F) ITT was conducted in fasted 16-wk-old male mice as described in the Materials and Methods, and AUC calculated ($n = 5$ to 10). *, $P < 0.05$; **, $P < 0.01$; ***, $P < 0.001$.

0.001) (Fig. 1F), suggesting that aggravated insulin resistance leads to the diabetes of male *Atg7* cKO-*ob/ob* mice. Blood glucose profile and body weight of female *Atg7* cKO-*ob/ob* mice were not significantly different from those of female *Atg7* cWT-*ob/ob* mice ($P > 0.1$) (Fig. S1, S2A). However, IPGTT and ITT showed tendency toward metabolic deterioration in female *Atg7* cKO-*ob/ob* mice compared to female *Atg7* cWT-*ob/ob* mice, while statistical significance was not reached ($P > 0.05$) (Fig. S2B, C). Since metabolic deterioration was more prominent in male *Atg7* cKO-*ob/ob* mice compared to female *Atg7* cKO-*ob/ob* mice, the subsequent experiments were conducted employing male *Atg7* cKO-*ob/ob* mice.

The insulinogenic index, representing β -cell response to changing glucose level, did not differ between *Atg7* cKO-*ob/ob* and *Atg7* cWT-*ob/ob* mice (Fig. S3A). β -cell mass was also not different between *Atg7* cKO-*ob/ob* and *Atg7* cWT-*ob/ob* mice (Fig. S3B), suggesting that aggravated β -cell failure might not play a dominant role in the development of diabetes in *Atg7* cKO-*ob/ob* mice. The metabolic profile of *Atg7* cKO-*ob/w* and *Atg7* cWT-*ob/w* mice was not different from that of *Atg7* cKO and *Atg7* cWT mice, respectively (Fig. S4). Hence, *Atg7* cKO-*ob/w* and *Atg7* cWT-*ob/w* mice were employed instead of *Atg7* cKO and *Atg7* cWT mice, respectively, in most of the following experiments.

Enhanced inflammasome activation in autophagy-deficient M ϕ s

We next studied the possible mechanism of overt diabetes and increased insulin resistance in *Atg7* cKO-*ob/ob* mice by

investigating the inflammasome activation in response to lipid injury, since inflammasome activation due to lipid injury has been implicated in obesity-induced diabetes^{9,10} and autophagy deficiency can enhance inflammasome activation.^{11,12} Primary peritoneal M ϕ s from control *Atg7* cWT mice were cultured with PA (palmitic acid) in combination with LPS (lipopolysaccharide), a condition that is capable of activating the inflammasome.¹⁰ While LPS alone induced only a minimal amount of IL1B (interleukin 1 β) release and PA alone had virtually no effect on IL1B release from peritoneal M ϕ s of *Atg7* cWT mice, significant IL1B release was observed when treated with PA in combination with LPS (Fig. 2A). IL1B release in response to PA in combination with LPS was significantly higher when M ϕ s from *Atg7* cKO mice were employed ($P < 0.05$ to 0.01) (Fig. 2A), suggesting increased inflammasome activation in autophagy-deficient M ϕ s. Indeed, western blot analysis demonstrated increased maturation of IL1B and increased activation of CASP1 (caspase 1) in autophagy-deficient M ϕ s treated with PA and LPS combination compared to autophagy-competent M ϕ s (Fig. 2B). These results show that autophagy deficiency promotes inflammasome activation in response to lipid injury which can aggravate insulin resistance associated with obesity.

We further investigated the mechanism of increased inflammasome activation in autophagy-deficient M ϕ s by studying the mitochondrial events that have been incriminated as crucial steps in inflammasome activation.²⁴ Furthermore, mitochondrial function and events during inflammasome activation are likely to be affected by autophagy deficiency since mitochondria are important target organelles of autophagy in a process called mitophagy.¹ While PA alone or LPS alone reduced the

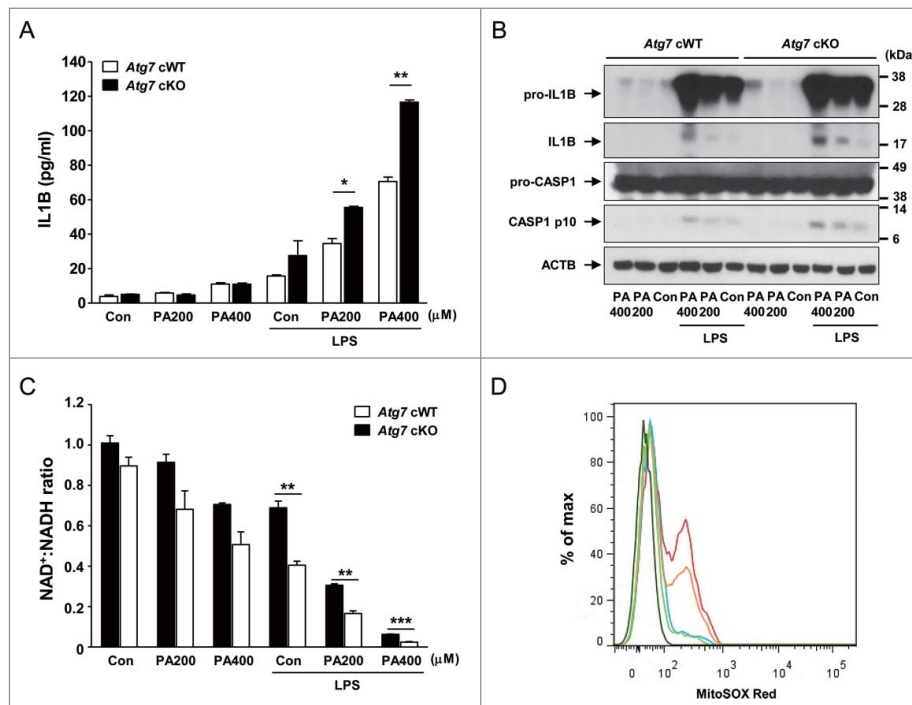


Figure 2. Inflammasome activation in M ϕ s from 12-wk-old mice by varying doses of PA in combination with 500 ng/ml LPS. (A) Primary peritoneal M ϕ s were incubated with PA of the indicated concentrations and LPS. After 24 h of culture, IL1B concentration in the supernatant was determined by ELISA. (B) After incubation of primary peritoneal M ϕ s with PA of the indicated doses and LPS for 24 h, cell extracts were subjected to western blot analysis using anti-IL1B and -CASP1 Abs. (C) After the same incubation of M ϕ s as in (B), NAD⁺:NADH ratio was determined using a commercial kit. (D) After the same incubation of M ϕ s as in (B), cells were incubated with MitoSOX Red for flow cytometry (dark green, unstained; green, *Atg7* cWT M ϕ s treated with 400 μ M PA; blue, *Atg7* cWT M ϕ s treated with LPS; orange, *Atg7* cWT M ϕ s treated with 400 μ M PA + LPS; red, *Atg7* cKO M ϕ s treated with 400 μ M PA + LPS). *, $P < 0.05$; **, $P < 0.01$; ***, $P < 0.001$.

ratio of oxidized to reduced nicotinamide adenine dinucleotide ($\text{NAD}^+:\text{NADH}$) to a small degree, treatment with PA in combination with LPS had profound effects on the $\text{NAD}^+:\text{NADH}$ ratio, suggesting obvious mitochondrial dysfunction after combined treatment with PA and LPS (Fig. 2C). Such decreases of $\text{NAD}^+:\text{NADH}$ ratio by PA in combination with LPS were further aggravated when autophagy-deficient M ϕ s were employed ($P < 0.01$ to 0.001) (Fig. 2C), supporting that autophagy deficiency is a proinflammatory condition facilitating inflammasome activation by lipid injury. We also studied mitochondrial ROS content that can be increased by mitochondrial dysfunction²⁵ and plays an important role in inflammasome activation by diverse effectors.²⁶ While LPS alone has minimal effects on the mitochondrial ROS content determined by MitoSOX Red staining,²⁵ mitochondrial ROS content was notably increased by PA in combination with LPS in autophagy-competent M ϕ s (Fig. 2D). Mitochondrial ROS content was further increased by PA in combination with LPS when autophagy-deficient M ϕ s were employed (Fig. 2D), supporting that mitochondrial dysfunction associated with autophagy deficiency can lead to increased mitochondrial ROS and enhanced inflammasome activation by lipid injury.

Enhanced adipose tissue inflammation of *Atg7* cKO-ob/ob mice

We next studied whether low-grade adipose tissue inflammation and inflammasome activation in vivo is altered in *Atg7* cKO-ob/ob mice that have deteriorated metabolic profile. Consistent with our hypothesis that myeloid cell-specific autophagy

deficiency is a proinflammatory condition associated with lipid injury, the numbers of CLS (crown-like structure) representing M ϕ aggregate around dead adipocytes and meta-inflammation associated with obesity,²⁷ were significantly higher in adipose tissue of *Atg7* cKO-ob/ob mice compared to *Atg7* cWT-ob/ob mice ($P < 0.01$) (Fig. 3A). Consistently, the expression of inflammatory markers such as *Tnf* (tumor necrosis factor), *Il6* (interleukin 6), pro-*Il1b* and *Adgre1* (adhesion G protein-coupled receptor E1) was significantly higher in the SVF (stromal vascular fraction) of white adipose tissue from *Atg7* cKO-ob/ob mice compared to *Atg7* cWT-ob/ob mice ($P < 0.05$ to 0.001) (Fig. 3B), indicating increased low-grade tissue inflammation as a cause of increased insulin resistance in *Atg7* cKO-ob/ob mice.

We next studied whether the increased adipose tissue inflammation in *Atg7* cKO-ob/ob mice is associated with inflammasome activation. Indeed, western blot analysis showed that maturation of IL1B from pro-IL1B and activation of CASP1 were more pronounced in the SVF of *Atg7* cKO-ob/ob mice compared to *Atg7* cWT-ob/ob mice (Fig. 3C), supporting the role of enhanced inflammasome activation associated with M ϕ s autophagy deficiency as a cause of increased adipose tissue inflammation in vivo. Probably because of increased inflammasome activation in vivo, serum IL1B level was significantly higher in *Atg7* cKO-ob/ob mice compared to *Atg7* cWT-ob/ob mice ($P < 0.05$) (Fig. 3D).

We also studied islet inflammation that could be affected by inflammasome activation associated with obesity.²⁸ Islet infiltration of ADGRE1⁺ M ϕ s in autophagy-competent *Atg7* cWT-ob/ob mice which was significantly higher compared to lean

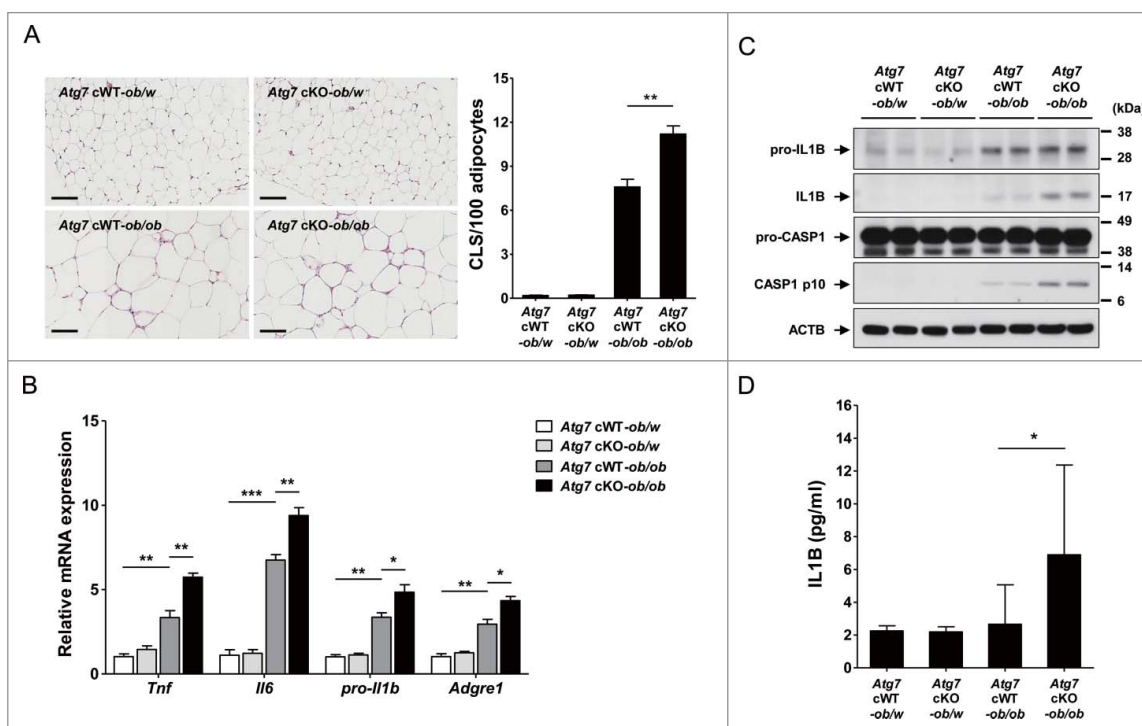


Figure 3. Inflammasome activation in vivo. (A) The number of CLS in white adipose tissue of 20-wk-old mice was counted as described in Materials and Methods ($n = 4$ each) (right). Representative H&E stained sections of white adipose tissue are shown (left, scale bar: $100 \mu\text{m}$). (B) Total mRNA was extracted from the SVF of white adipose tissue from 20-wk-old mice, and quantitative RT-PCR was done using primers specific for *Tnf*, *Il6*, pro-*Il1b* and *Adgre1* ($n = 3$ each). (C) Tissue lysate of the SVF was subjected to western blot analysis using anti-IL1B and -CASP1 Abs. (D) Serum IL1B level was determined using a commercial ELISA kit ($n = 3$ to 15). *, $P < 0.05$; **, $P < 0.01$; ***, $P < 0.001$.

mice, was further augmented in *Atg7* cKO-*ob/ob* mice ($P < 0.05$) (Fig. S5), suggesting that inflammation in myeloid cell-specific autophagy deficiency occurs in both insulin target tissues and islets producing insulin. More pronounced islet inflammation in *Atg7* cKO-*ob/ob* mice compared to *Atg7* cWT-*ob/ob* mice might account for the absence of compensatory increase of β -cell function despite increased insulin resistance in *Atg7* cKO-*ob/ob* mice compared to *Atg7* cWT-*ob/ob* mice (see Fig. S3A), while β -cell dysfunction is not a dominant factor in the development of diabetes in *Atg7* cKO-*ob/ob* mice.

Regulatory T (Treg) cells in *Atg7* cKO mice

We next studied Treg cells that can modulate low-grade inflammation associated with insulin resistance²⁹ and can be affected by cytokines such as IL1B.^{30,31} When we measured the Treg cell fraction in the SVF of white adipose tissue from *Atg7* cWT-*ob/ob* mice, the percentage of FOXP3 (forkhead box P3)⁺ CD4⁺ Treg cells among CD3E⁺ T cells was significantly suppressed compared to *Atg7* cWT-*ob/w* mice ($P < 0.01$) (Fig. 4A), supporting reduced Treg cell activity as a factor in the augmented adipose tissue meta-inflammation.²⁹ In the SVF of *Atg7* cKO-*ob/ob* mice, the percentage of FOXP3⁺ CD4⁺ Treg cells among CD3E⁺ T cells was further suppressed compared to *Atg7* cWT-*ob/ob* mice ($P < 0.05$) (Fig. 4A), suggesting that suppressed Treg cell activity contributes to the further

augmented adipose tissue inflammation and insulin resistance in *Atg7* cKO-*ob/ob* mice. When we examined IL2RA (interleukin 2 receptor, α chain) expression that reflects the suppressive function of Treg cells,³² the percentage of FOXP3⁺ IL2RA⁺ Treg cells among CD3E⁺ T cells was again further suppressed in the SVF of white adipose tissue from *Atg7* cKO-*ob/ob* mice compared to *Atg7* cWT-*ob/ob* mice ($P < 0.05$), which was already lower than that from lean *Atg7* cWT-*ob/w* mice ($P < 0.01$) (Fig. 4B). The numbers of FOXP3⁺ CD4⁺ CD3E⁺ Treg cells and FOXP3⁺ IL2RA⁺ CD3E⁺ Treg cells in the SVF of white adipose tissue from *Atg7* cKO-*ob/ob* mice were also significantly lower than those from *Atg7* cWT-*ob/ob* mice ($P < 0.05$ for both comparisons), which were already lower than those from lean *Atg7* cWT-*ob/w* mice ($P < 0.05$ for both comparisons) (Fig. 4A and B). In contrast, Treg cell activity was not different between them ($P > 0.1$) (Fig. S6), suggesting that changes in the number and proportion rather than activity of individual FOXP3⁺ IL2RA⁺ CD4⁺ Treg cell contribute to the disparate degree of adipose tissue meta-inflammation between groups.

Colitis in *Atg7* cKO mice

Since M ϕ s are important players in mucosal immunity of gut³³ and autophagy is an important factor in the development of IBD,²² we also studied whether susceptibility to experimental

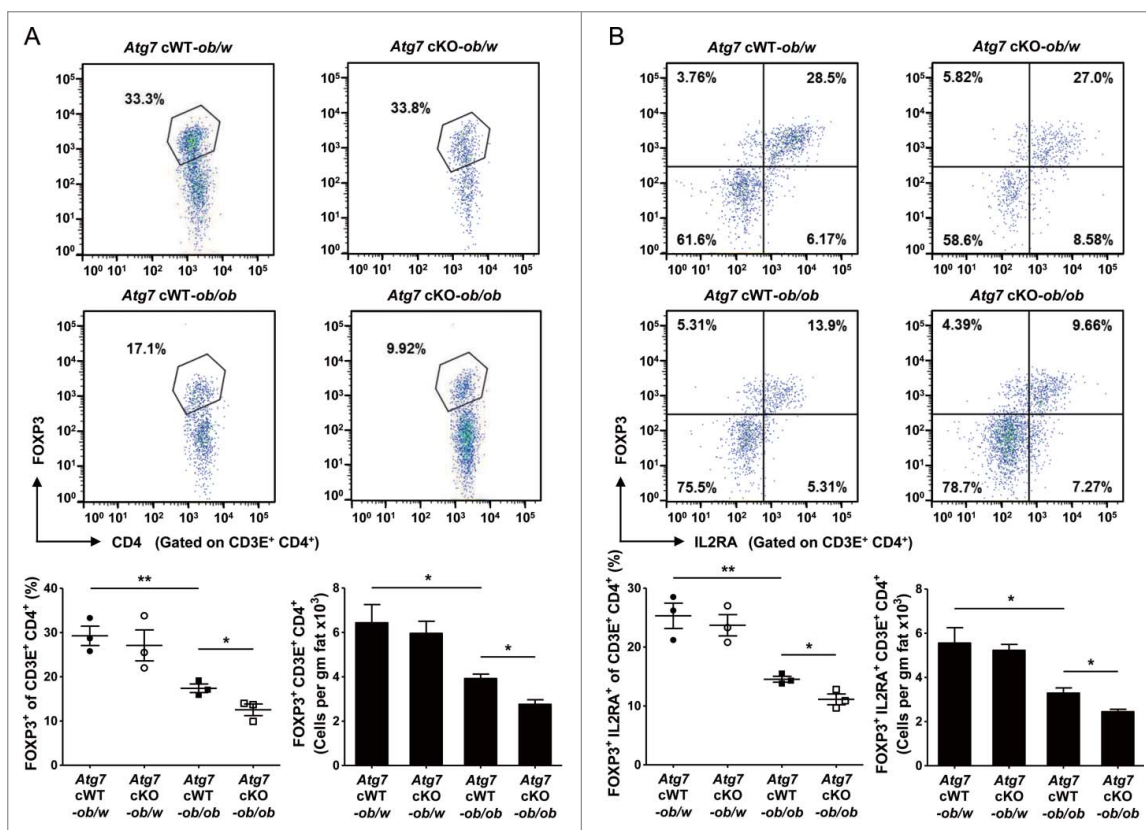


Figure 4. Treg cells in white adipose tissue. (A) Cells in the SVF of white adipose tissue from 20-wk-old mice were incubated with a mixture of anti-CD3E, -CD4, and -IL2RA Abs, and then with -FOXP3 Ab as described in Materials and Methods. FOXP3 and CD4 expression was examined by flow cytometry gated on CD3E⁺ CD4⁺ cells. The proportions of FOXP3⁺ cells among CD3E⁺ CD4⁺ cells (lower left) and the numbers of FOXP3⁺ CD3E⁺ CD4⁺ cells/gm adipose tissue (lower right) ($n = 3$ each). Representative FACS scattergrams are shown (upper). (B) Cells were incubated with Abs as in (A), and FOXP3 and IL2RA expression was examined by flow cytometry gated on CD3E⁺ CD4⁺ cells. The proportions of FOXP3⁺ IL2RA⁺ cells among CD3E⁺ CD4⁺ cells (lower left) and the numbers of FOXP3⁺ IL2RA⁺ CD3E⁺ CD4⁺ cells/gm adipose tissue (lower right) ($n = 3$ each). Representative FACS scattergrams are shown (upper). *, $P < 0.05$; **, $P < 0.01$.

colitis is altered in *Atg7* cKO mice. Weight loss after treatment with 2.5% DSS (dextran sodium sulfate) was more severe in *Atg7* cKO mice compared to *Atg7* cWT mice ($P < 0.05$) (Fig. 5A). Colon length measured 7 d after DSS administration was also significantly shorter in *Atg7* cKO mice compared to *Atg7* cWT mice ($P < 0.05$), suggesting more pronounced colitis in *Atg7* cKO mice (Fig. 5B). The difference in body weight after 2.5% DSS treatment between *Atg7* cKO and *Atg7* cWT mice disappeared when antibiotics were administered since 2 d before 2.5% DSS treatment, indicating the role of intestinal microbiota as incriminating agents causing aggravated colitis in *Atg7* cKO mice after DSS administration (Fig. 5A). Probably because of aggravated colitis, survival was significantly decreased in *Atg7* cKO mice compared to *Atg7* cWT mice after administration of 4% DSS that has been employed to study the mortality of mice due to colitis³⁴ ($P < 0.01$) (Fig. 5C).

Colitis scoring of H&E sections showed more severe colitis in *Atg7* cKO mice compared to *Atg7* cWT mice ($P < 0.05$) (Fig. 6A), consistent with the more severe weight loss and decreased survival of *Atg7* cKO mice. When we examined the expression of cytokines³⁵⁻³⁸ and chemokines³⁹⁻⁴¹ that can be effector molecules in aggravated colitis using colonic mRNA prepared from paraffin-embedded colonic sections, mRNA expression of pro-*Il1b*, *Ccl2* (chemokine (C-C motif) ligand 2) and *Cxcl1* (chemokine (C-X-C motif) ligand 1) was significantly elevated in colon tissue of *Atg7*

cKO mice treated with 2.5% DSS compared to *Atg7* cWT mice treated in the same way ($P < 0.05$), while the expression of other cytokines such as *Il6* or *Tnf* and that of chemokines such as *Ccl5* (chemokine (C-C motif) ligand 5) was marginally elevated ($P > 0.05$). The expression of *Tgfb* (transforming growth factor, β) in the colonic tissues was not different between *Atg7* cKO and *Atg7* cWT mice ($P > 0.1$) (Fig. 6B). We also studied Th (T helper) cells skewing that can affect the development of colitis.^{38,42,43} We observed significantly increased proportion of IFNG (interferon gamma)⁺ Th1 cells in the colonic lamina propria of *Atg7* cKO mice compared to *Atg7* cWT mice ($P < 0.05$). In contrast, the proportion of IL17A (interleukin 17A)⁺ Th17 cells was not significantly different between the 2 mouse groups ($P > 0.1$) (Fig. 6C), which could be attributable to the absence of a significant increase of *Tgfb* expression in colonic tissue of *Atg7* cKO mice, a critical component of the Th17 response.⁴⁴ Infiltration of ADGRE1⁺ ITGAM (integrin α M)/CD11b⁺ myeloid cells was more pronounced in the lamina propria of *Atg7* cKO mice compared to *Atg7* cWT mice as evidenced by significantly increased percentage of ADGRE1⁺ ITGAM⁺ myeloid cells in the lamina propria of *Atg7* cKO mice compared to *Atg7* cWT mice ($P < 0.05$) (Fig. S7A); however, the proportion of Treg cells was not significantly different between the 2 mouse groups ($P > 0.1$) (Fig. S7B).

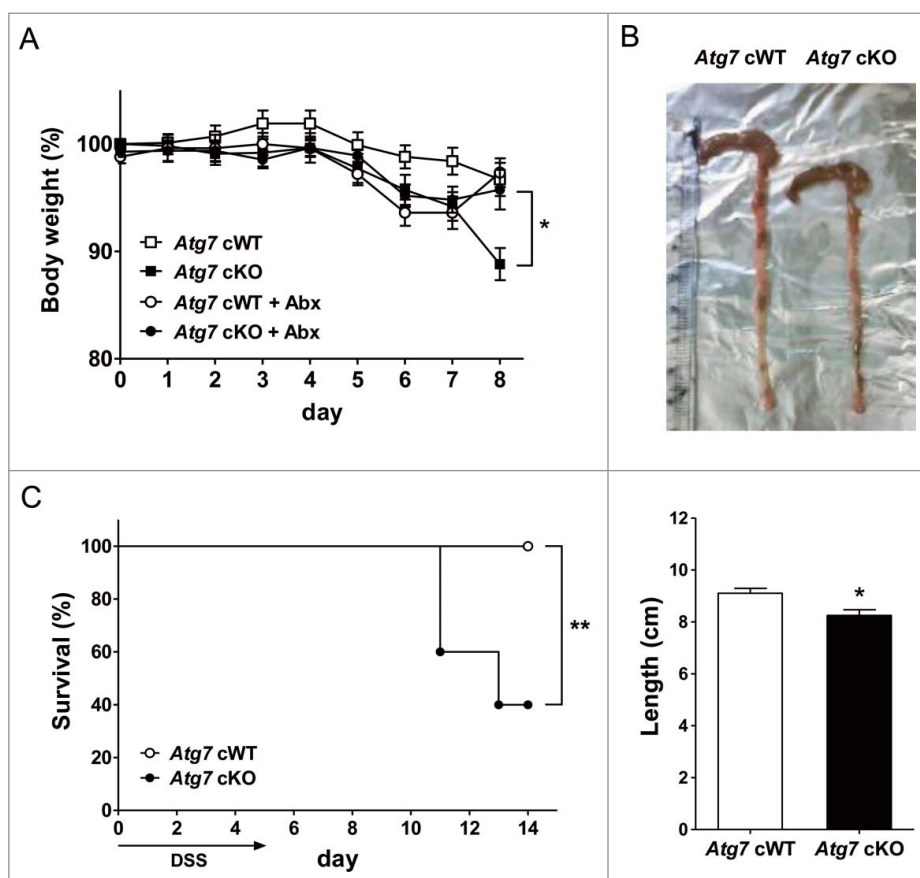


Figure 5. DSS-induced colitis in *Atg7* cKO mice. (A) Body weight was monitored during and after oral administration of 2.5% DSS for 5 d ($n = 7$ each). The antibiotic mixture (Abx) was administered since 2 d before DSS as described in Materials and Methods, and body weight monitored ($n = 7$ each). (B) Gross morphology (upper) and length (lower) of the colons on day 7 of DSS administration ($n = 5$ to 6). (C) Survival after administration of 4% DSS was monitored as described in Materials and Methods ($n = 10$ each). *, $P < 0.05$; **, $P < 0.01$.

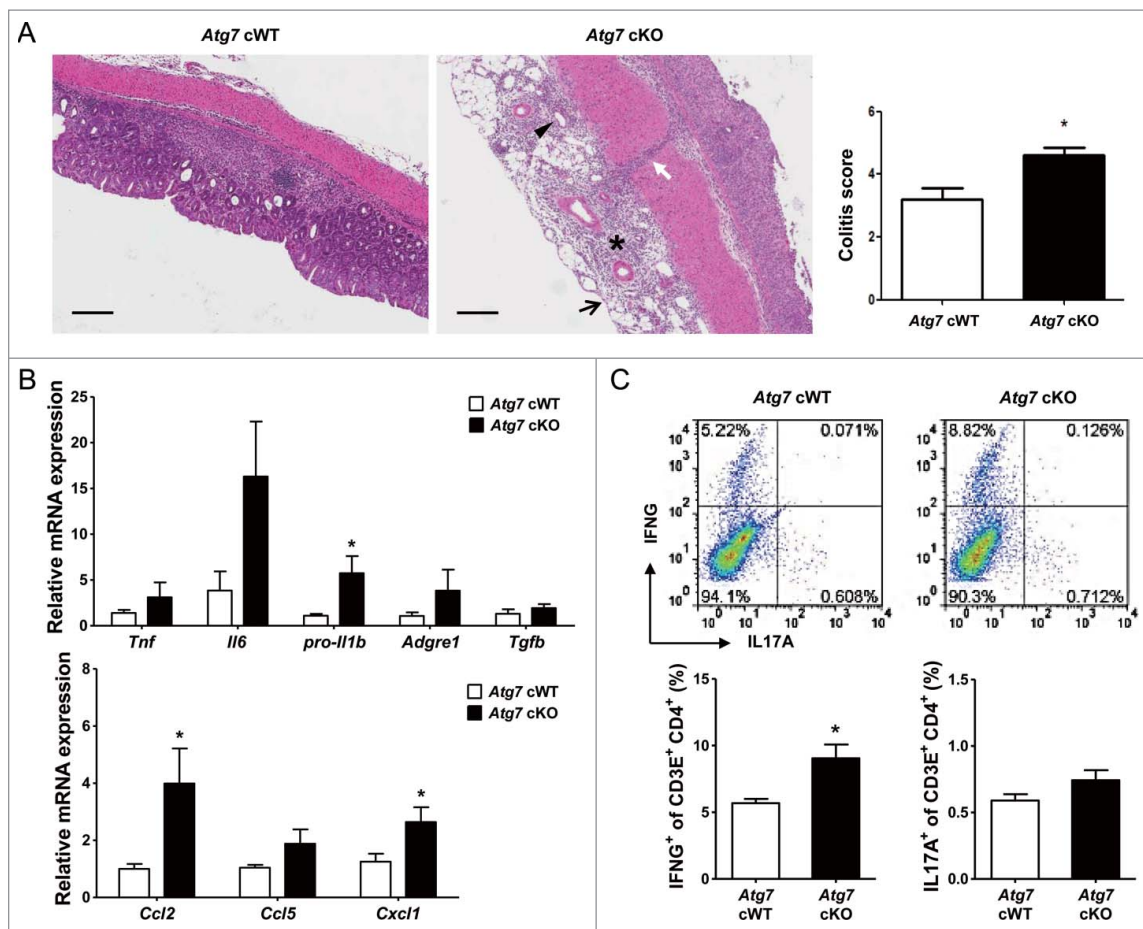


Figure 6. Inflammation and Th1 skewing in the colon of *Atg7* cKO mice. (A) Colitis score was calculated on d 7 of DSS treatment as described in Materials and Methods ($n = 5$ each) (right). Representative H&E sections are shown (left, scale bar: 200 μm) (asterisk, inflammation; arrow, ulceration; arrow head, regeneration; white arrow, transmural lesion). (B) Relative expression of cytokines and chemokines in the colonic tissues on d 7 of DSS treatment assessed by quantitative RT-PCR analysis of mRNA prepared using a formalin-fixed paraffin-embedded extraction kit ($n = 8$ to 10). (C) Th skewing in the colonic lamina propria on day 7 of DSS treatment was evaluated by flow cytometry. The proportions of IFNG⁺ cells and IL17A⁺ cells among CD3E⁺ CD4⁺ T cells (lower) ($n = 4$ each). Representative scattergrams are shown (upper). *, $P < 0.05$.

We next studied whether aggravated colitis in *Atg7* cKO mice after DSS treatment leads to systemic infection or inflammation across the colonic tissue. Serum levels of IL1B after DSS treatment were significantly increased in *Atg7* cKO mice compared to *Atg7* cWT mice, suggesting augmented systemic inflammation probably due to the impaired gut barrier function after DSS treatment of *Atg7* cKO mice ($P < 0.05$) (Fig. 7A). Serum levels of IL6 and TNF after DSS treatment appeared to be increased in *Atg7* cKO mice compared to *Atg7* cWT mice, while statistical significance was not reached ($P > 0.05$) (Fig. 7A). Since evidence of systemic inflammation suggested the possibility of systemic infection, we studied the presence of bacterial 16S rRNA genes in the liver and systemic lymphoid organ. The content of bacterial 16S rRNA genes was significantly increased in the liver of *Atg7* cKO mice compared to *Atg7* cWT mice ($P < 0.05$) (Fig. 7B), suggesting increased bacterial invasion into the liver parenchymal tissue of *Atg7* cKO mice. The content of bacterial 16S rRNA genes also appeared to be increased in the mesenteric lymph nodes and spleen of *Atg7* cKO mice compared to *Atg7* cWT mice, while the statistical significance was not reached ($P > 0.05$) (Fig. 7B).

Discussion

We observed that myeloid cell-specific autophagy is an important element in the modulation of adipose tissue inflammation and insulin resistance associated with lipid injury. While the susceptibility of mice with myeloid cell-specific disruption of essential autophagy genes to infectious agents has been widely studied,^{45,46} metabolic abnormalities associated with myeloid cell-specific autophagy deficiency have not been clearly shown. A recent paper reports that myeloid cell-specific *Atg5* deletion leads to increased tissue inflammation and injury specifically in the liver after high-fat diet feeding in combination with LPS administration.⁴⁷ However, the role of myeloid cell autophagy in metainflammation of tissues other than liver or in the development of T2D has not been demonstrated. The glucose profile of *Atg5* cKO mice fed high-fat diet is not higher than that of *Atg5* cWT mice fed high-fat diet.⁴⁷ The dissimilar glucose profile between *Atg5* cKO mice fed high-fat diet and *Atg7* cKO-*ob/ob* mice appears to be due to the difference between high-fat diet and obesity due to *Lep* knockout in *ob/ob* mice. Obesity due to LEP deficiency can impose more severe metabolic stress compared to high-fat diet. LEP deficiency may cause additional metabolic or immunological abnormalities that are not seen in

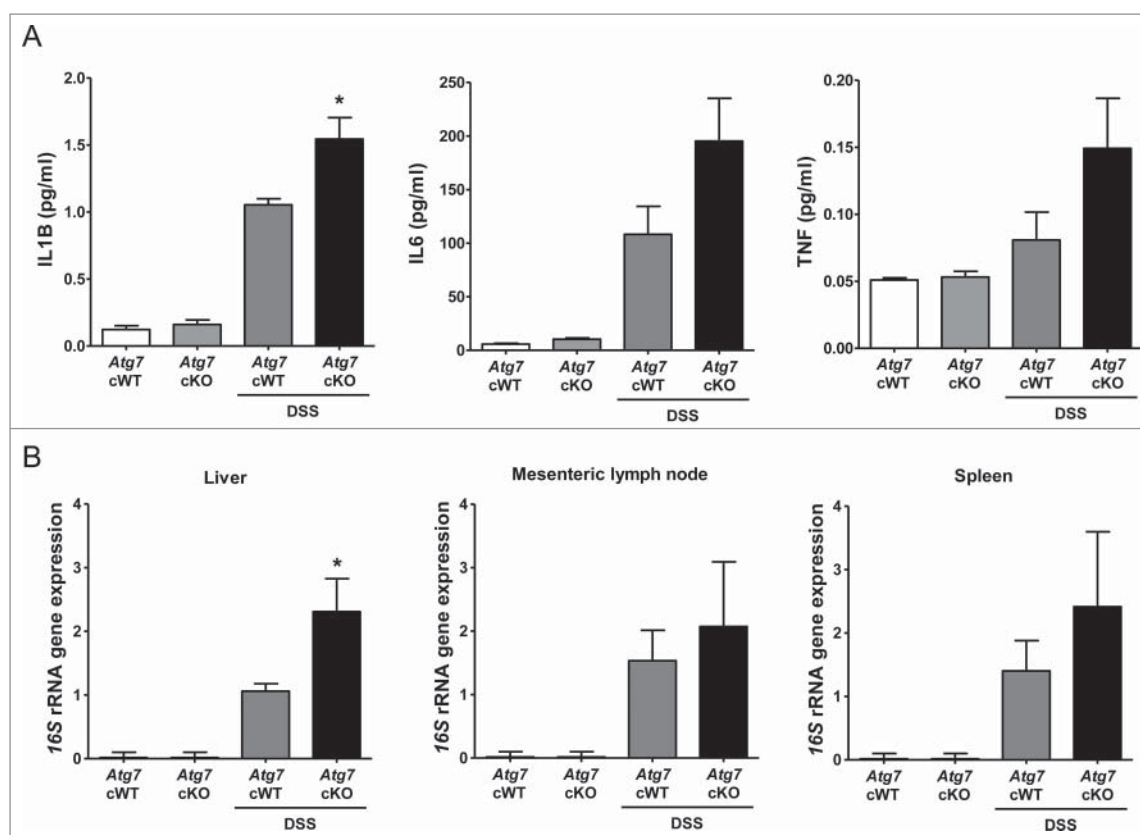


Figure 7. Systemic inflammation and bacterial invasion after DSS treatment. (A) Serum levels of cytokines after DSS treatment were determined by ELISA ($n = 6$ each). (B) Relative expression of bacterial *16S* rRNA genes in the liver, mesenteric lymph node and spleen determined by quantitative PCR as described in Materials and Methods ($n = 9$ each). *, $P < 0.05$.

mice fed high-fat diet.⁴⁸ Here, we clearly show that myeloid cell-specific autophagy deficiency led to the development of T2D in obese mice that otherwise did not develop overt T2D. Myeloid cells that play dominant roles in the development of obesity-induced diabetes appear to be *Mφs* as was shown in the current in vitro investigation. However, the role of other myeloid cells such as dendritic cells or granulocytes that are target cells of *Cre*-mediated gene deletion in *Atg7* cKO mice⁴⁹ cannot be totally eliminated, as both granulocytes and dendritic cells participate in the insulin resistance associated with obesity.^{50,51}

The development of T2D in *Atg7* cKO-*ob/ob* mice but not in lean *Atg7* cKO mice suggests that autophagy-deficient myeloid cells do not display significant inflammatory phenotypes in the basal state, but show proinflammatory features in the presence of activators of inflammation or metabolic stress. Thus, autophagy-deficient *Mφs* appear to be susceptible to inflammasome activators such as lipids, which is the reason *Atg7* cKO mice show increased inflammatory features and overt T2D when they become obese. Previous papers show that lipids such as fatty acids or cholesterol are efficient activators of the inflammasome complex.^{6,10,52} While the detailed molecular mechanism of lipid-induced inflammasome activation remains to be investigated, mitochondrial dysfunction induced by fatty acids in combination with LPS likely plays an important role in inflammasome activation, which was exemplified by the markedly decreased $\text{NAD}^+:\text{NADH}$ ratio and increased mitochondrial ROS content, consistent with previous papers.^{12,24} An in vivo source of TLR (toll-like receptor) ligands which are

essential for efficient stimulation of inflammasome in addition to lipid, could be a low-level endotoxin owing to altered intestinal barrier function^{53,54} or AHSG (α -2-HS-glycoprotein) that can activate TLR in complex with lipids.⁵⁵ All these results suggest that inflammasome activation due to lipid or obesity could be a crucial event in obesity-induced insulin resistance by enhancing the release of IL1B as an effector molecule of insulin resistance, which can be exacerbated by autophagy deficiency of myeloid cells. However, as deficiency of IL18, another product of inflammasome or NLRP3 activation, has been reported to induce obesity and insulin resistance,⁵⁶ general role of inflammasome or NLRP activation in the pathogenesis of metabolic syndrome and T2D still remains to be clarified.

The main mechanism of T2D in *Atg7* cKO-*ob/ob* mice appears to be aggravated insulin resistance due to increased inflammasome activation and increased IL1B production associated with autophagy deficiency. Furthermore, a suppressed Treg cell fraction in the SVF of white adipose tissue from *Atg7* cKO-*ob/ob* mice compared to *Atg7* cWT-*ob/ob* mice might also contribute to augmented tissue inflammation and insulin resistance in insulin target tissues such as adipose tissue.²⁹ The mechanism of a further decrease in Treg cells in white adipose tissue of *Atg7* cKO-*ob/ob* mice is not clear, and may involve degradation of mature IL33 by increased production of active CASP1.⁵⁷ A recent paper reported decreased glucose utilization by expansion of adipose tissue Treg cells in age-associated insulin resistance; however, such findings may not be relevant in obesity-associated insulin resistance.⁵⁸

Previous papers have reported that IL1B blockade improves glucose homeostasis by reducing insulin resistance and enhancing β -cell function.^{59,60} In contrast, the role of deteriorated β -cell function in the development of diabetes in *Atg7* cKO-*ob/ob* mice was not evident. Since the oligomer of amyloidogenic human-type IAPP (islet amyloid polypeptide) but not nonamyloidogenic murine IAPP can induce inflammasome activation,⁶¹ the role of inflammasome activation with or without autophagy deficiency may be more prominent in human T2D rather than murine T2D.^{61,62} While impairment of β -cell function may not be the primary cause of diabetes in *Atg7* cKO-*ob/ob* mice, the insulinogenic index was not further increased in *Atg7* cKO-*ob/ob* mice compared to *Atg7* cWT-*ob/ob* mice despite aggravated insulin resistance, suggesting that β -cell response to increased insulin resistance was not adequate in *Atg7* cKO-*ob/ob* mice. More pronounced islet inflammation in *Atg7* cKO-*ob/ob* mice compared to *Atg7* cWT-*ob/ob* mice might be responsible for such an insufficient response to insulin resistance.

Previous papers report exacerbation of experimental colitis in mice with systemic autophagy insufficiency or after transplantation of autophagy-deficient hematopoietic cells.^{36,63,64} Here, we directly demonstrated aggravated experimental colitis in myeloid cell-specific autophagy-knockout mice, leading to increased mortality. In addition, we observed apparently increased colonic tissue expression of pro-*Il1b* and *Il6* that are important players in colitis of DSS-treated *Atg7* cKO mice compared to *Atg7* cWT mice,³⁶⁻³⁸ while the induction of *Il6* was marginal. The expression of chemokines such as *Ccl2* and *Cxcl1* was also upregulated in the colon of DSS-treated *Atg7* cKO mice, which is consistent with their role in chemotaxis and colitis.^{39,41} Aggravated inflammation in DSS-treated *Atg7* cKO mice compared to *Atg7* cWT mice might be related to the recently reported colitogenic role of IL18 that can be produced through the inflammasome in DSS-induced colitis.⁶⁵ We also observed skewing toward Th1 in colonic lamina propria of DSS-treated *Atg7* cKO mice compared to *Atg7* cWT mice. Th17 skewing was not observed in colonic lamina propria of DSS-treated *Atg7* cKO mice despite the increased expression of pro-*Il1b* and *Il6* that are important components in Th17 differentiation,^{44,66} which could be due to the absence of *Tgfb* induction in colonic lamina propria of DSS-treated *Atg7* cKO mice. *Tgfb* has been reported as an indispensable factor in Th17 skewing.^{44,66} While Th17 cells are important in diverse IBD models,^{67,68} recent papers show a critical role for Th1 cells rather than Th17 cells as effectors in DSS-induced colitis.^{69,70} In addition to the upregulated expression of cytokines in the colonic tissue, serum levels of IL1B were also elevated in DSS-treated *Atg7* cKO mice compared to *Atg7* cWT mice, suggesting systemic inflammation probably due to the impaired gut barrier function after DSS treatment particularly in *Atg7* cKO mice. Serum levels of IL6 and TNF appeared increased in DSS-treated *Atg7* cKO mice, while statistical significance was marginal. Since evidence of systemic inflammation suggested the possibility of systemic microbial invasion, we studied the presence of bacterial 16S rRNA genes in the liver and lymphoid organ. The content of bacterial 16S rRNA genes was significantly increased in the liver of DSS-treated *Atg7* cKO mice compared to *Atg7* cWT mice, suggesting bacterial invasion of the liver

parenchymal tissue probably through the portal vein. These results indicate that autophagy deficiency in myeloid cells of the intestine predispose the host to the systemic infection and sepsis when the intestinal barrier is disrupted.

Altogether, these results suggest that autophagy deficiency in myeloid cells is a factor not only in the progression from obesity to diabetes and but also in colitis. The western diet that has been incriminated as a cause of pandemics of metabolic syndrome is also a risk factor for IBD.²³ Since lipid is a target of autophagy and in turn affects autophagy,^{1,5} lipid excess in conjunction with autophagy dysfunction due to aging or genetic predisposition could be a common cause of metabolic syndrome and colitis, and autophagy modulators may have a therapeutic potential against these diseases.

Materials and methods

Mice

To generate *Atg7* cKO mice with myeloid cell-specific deletion of *Atg7*, an essential autophagy gene, *Atg7* cWT mice (kindly provided by Dr. Komatsu at Niigata University, Japan) of the C57BL/6 background were crossed with *Lys-Cre* mice with myeloid cell-specific Cre recombinase expression owing to targeted insertion of the *Cre* cDNA into the lysozyme M locus (Jackson Laboratory).⁴⁹ *Cre*-mediated deletion of *Atg7* was confirmed by PCR using genomic DNA from peritoneal M ϕ s and primers flanking the floxed region as previously reported.¹⁴ *Atg7* cKO-*ob/ob* mice were generated by crossing *Atg7* cKO mice to *ob/w* (heterozygous *Lep* knockout) mice twice. Blood glucose levels were determined using a One Touch glucometer (Lifescan Inc., Chesterbrook, PA, USA). We defined 'diabetes' as a single measurement of nonfasting blood glucose level above 17.6 mM or 3 consecutive measurement of nonfasting blood glucose level above 12.8 mM. IPGTT and ITT were performed by injecting 1 g/kg glucose (Amresco, 0188) to overnight fasted mice and injecting 0.75 U/kg of regular insulin (Lilly, HI0210) to mice fasted for 6 h, respectively.^{14,71} To calculate the relative β -cell mass, point counting morphometry was performed after insulin immunohistochemistry of more than 3 parallel sections of different cut levels containing more than 30 pancreatic islets.¹⁴ The insulinogenic index was calculated as $(\Delta\text{insulin}_{15\text{ min}} / \Delta\text{glucose}_{15\text{ min}})$.¹⁴

Experimental colitis was induced by the administration of 2.5 to 4.0% (w/v) DSS (MP Biologicals, 02160110) dissolved in sterile distilled water for 5 d. On day 3, the DSS solution was replaced with a fresh solution. On d 7, mice were sacrificed for colitis assessment. To study the role of intestinal microbiota in colitis, antibiotic mixture consisting of vancomycin (10 mg/kg; Sigma, V2002), neomycin (30 mg/kg; Sigma, N6386), carbenicillin (50 mg/kg; Sigma, C1389), and metronidazole (50 mg/kg; Sigma, M3761) was administered orally every day since 2 d before DSS administration for a total of 9 d.

All animal experiments were conducted in accordance with the Public Health Service Policy in Humane Care and Use of Laboratory Animals. Mouse experiments were approved by the IACUC of Samsung Medical Center Animal Facility, an AAA-LAC-accredited unit.

M ϕ isolation

Primary peritoneal M ϕ s were isolated from 2- to 3-mo-old mice 3 d after intraperitoneal injection of 3.85% thioglycollate (Becton Dickinson, 4311260), and were then plated on culture plates for incubation at 37°C overnight.⁷² After removal of nonadherent cells by repeated washing, adherent cells were cultured in RPMI 1640 (Lonza, 12-702F) supplemented with 10% fetal bovine serum (FBS; Gibco, 16000-044), 2 mM L-glutamine (Lonza, 17-605E) and 100 IU/ml penicillin-streptomycin (Lonza, 17-745E) for further experiments.

ELISA

Serum insulin levels before and 15 min after 1g/kg glucose challenge were determined using an ELISA kit (Shibayagi Co., AKRIN-011T) to calculate the insulinogenic index, as above. IL1B levels in the culture supernatant were measured using an ELISA kit from R&D Systems. Serum IL1B, IL6 and TNF levels were determined using ELISA kits (R&D Systems, DY401, DY406, and DY410, respectively).

Western blotting

Western blot analysis was performed as previously described using anti-ATG7 (Cell Signaling Technology, 2631), -MAP1LC3A/B (Novus Biologicals, NB 100-2331), -SQSTM1 (Progen Biotechnik, GP62-C), -IL1B (Santa Cruz Biotechnology, SC-7884), -CASP1 p10 (Santa Cruz Biotechnology, SC-514) and -ACTB (actin, β ; Santa Cruz Biotechnology, SC-47778) Abs (antibodies).

RT-PCR

RNA was prepared from cells or tissues using TRIzol Reagent (Ambion, 15596018). RNA from paraffin-embedded tissue blocks was prepared using a formalin-fixed paraffin-embedded kit (Qiagen, 56404). cDNA was synthesized using M-MLV reverse transcriptase (Promega, M17013) and oligo(dT)₁₂₋₁₈ primer. The expression of *Atg7*, *Tnf*, *Il6*, *pro-Il1b*, *Adgre1*, *Tgfb*, *Ccl2*, *Ccl5*, *Cxcl1* and *Actb* was assessed by quantitative PCR using specific primer sets. Quantitative RT-PCR based on SYBR Premix EX Taq™ (Takara, RR420A) was carried out using the QuantStudio3 (Applied Biosystems, Waltham, MA, USA).

ROS content and NAD⁺:NADH ratio

Mitochondria-specific ROS was determined by flow cytometry using a FACSCalibur flow cytometer (BD Biosciences, San Jose, CA, USA) after staining with 5 μ M MitoSOX™ Red (Invitrogen, M36008) for 10 min at 37°C.²⁵ NAD⁺:NADH ratio was determined using a commercial kit (BioVision, K337-100) according to the manufacturer's recommendation.

Stromal vascular fraction (SVF)

For isolation of the SVF, epididymal adipose tissue representing visceral adipose tissue was cut into small pieces of

approximately 2 mm. After incubation in a 2 mg/ml type 2 collagenase solution (Worthington Biochemical, LS004174) at 37°C in a water bath for 45 min, digested tissue was centrifuged at 1,000 g for 8 min. After filtering through a 70 μ m mesh and RBC lysis, SVF was suspended in a DPBS (Dulbecco Phosphate Buffered Saline; Welgene, LB 001-02) supplemented with 2% BSA (Roche, 10 775 835 001), 2 mM EDTA (Cellgro, 46-034-CI) for further experiments.

Treg cells and FACS

Treg cell fraction of the SVF of adipose tissue was determined as published.⁵⁴ In brief, after filtering and RBC lysis of the resuspended SVF pellet as above, cells in the SVF were resuspended in FACS buffer (2 mM EDTA, 2% FBS in DPBS). After Fc blocking, cells were incubated with a mixture of anti-CD3E, -CD4 and -IL2RA Abs (eBioscience, 12-0031-82, 12-0042082, and 12-0251-82, respectively) in FACS buffer at 4°C for 30 min. After permeabilization, cells were incubated with anti-mouse/rat FOXP3 (FJK-16s) Ab (eBioscience, 12-5773-82) at 4°C for 30 min, and then triple-color flow cytometry was performed using a FACSVerse flow cytometer (BD Biosciences, San Jose, CA, USA). Data were analyzed with FlowJo software (Tree Star, Inc., Ashland, OR, USA). Suppressiveness activity of Treg cells was determined as described with modifications.⁷³ After RBC lysis of SVF cells, CD4⁺ IL2RA⁺ Treg cells were obtained using a MACS Regulatory T cell isolation kit (Miltenyl Biotech, 130-091-041) according to the manufacturer's recommendation. In brief, CD4⁺ T cells were purified by negative-selection method depleting non-CD4⁺ T cells. CD4⁺ T cells were labeled with PE-conjugated anti-IL2RA Ab and, next with anti-PE microbeads (Miltenyl Biotech, 130-091-041) for positive selection of CD4⁺ IL2RA⁺ cells using a magnetic column. Non-CD4⁺ T cells and CD4⁺ IL2RA⁻ cells were obtained from the spleen of C57BL/6 mice using the same methods to be used as APCs (antigen-presenting cells) and Teff (T effector) cells, respectively. Graded numbers of CD4⁺ IL2RA⁺ Treg cells were cocultured with 5 \times 10⁴ CD4⁺ IL2RA⁻ T cells labeled with 5 μ M CFSE (carboxyfluorescein succinimidyl ester; eBioscience, 65-0850) for 5 min and 1 \times 10⁵ APCs irradiated 30 Gy (X-RAD 320, North Branford, CT, USA) in the presence of 1 μ g/ml soluble anti-CD3E Ab (BD Pharmingen, 553057) for a total of 3 d. Cells were analyzed for CFSE dilution by flow cytometry.

To evaluate T helper skewing in colitis, large intestines were opened longitudinally and washed in ice-cold DPBS. After washing with DPBS, tissues were transferred to flask containing 10% FBS, 10mM EDTA in DPBS. After vigorous shaking, tissues were passed through a strainer. Tissues were then minced in 10 ml RPMI 1640 containing 0.5 mg collagenase D (Roche, 11 088 866 001) and DNase I (Roche, 11 284 932 001). After stirring for 20 min at 37°C, the supernatant fraction was collected for a total of 3 times. After centrifugation at 520 g for 5 min, the cell pellet was washed and resuspended in RPMI containing 2% FBS. Colonic lamina propria mononuclear cells were purified on a 40%/75% Percoll (GE Healthcare Life Sciences, 17-0891-01) gradient by centrifugation at 25°C, 930 g for 20 min. Cells were resuspended in FACS buffer. After Fc blocking with anti-mouse FCGR3/CD16 and FCGR2B/CD32

(eBioscience, 14-0161-85), cells were incubated with a mixture of anti-CD3E and -CD4 in FACS buffer at 4°C for 30 min. Cells were stimulated with phorbol 12-myristate 13-acetate (Sigma, P8139), ionomycin (Sigma, I9657) and GolgiStop (BD Biosciences, 554724) for 5 h. After washing, cells were incubated with anti-IL17A (eBioscience, 11-7177-81) and -IFNG Ab (eBioscience, 12-7311-82) at 4°C for 30 min. Samples were acquired on a FACSCalibur flow cytometer (BD Biosciences, San Jose, CA, USA) equipped with CellQuest software (BD Biosciences). Data were analyzed with FlowJo software (Tree Star, Inc.).

Histology

In adipose tissue, M ϕ aggregates containing up to 15 M ϕ s surrounding each adipocyte were considered as CLSs, and the number of CLSs per 100 adipocytes was counted as described.⁷⁴ To evaluate colitis, the colons were washed, fixed in 10% buffered formaldehyde, and embedded in paraffin for H&E staining. The degree of inflammation (score 0 to 3) was evaluated by a pathologist in a blinded fashion (occasional inflammatory cells in the lamina propria = 0; increased number of inflammatory cells in the lamina propria = 1; confluence of inflammatory cells extending into the submucosa = 2; and transmural extension of the infiltrate = 3). The degree of tissue damage was evaluated in the same manner (no mucosal damage = 0; lymphoepithelial lesion = 1; surface mucosal erosion or focal ulceration = 2; and extensive mucosal damage and extension into deeper structure = 3). Summation of inflammation and tissue damage scores were designated as the colitis score (0 to 6).³⁴

DNA extraction and quantification of bacteria by quantitative PCR

The liver, spleen and mesenteric lymph nodes were obtained from mice 7 d after DSS treatment, and immediately frozen and stored at -80°C. Genomic DNA was extracted from 0.5 g of each sample using a DNA extraction method.⁷⁵ Proteinase K (GeneAll Biotechnology, 392-001) was added in the cell lysis step. Total bacterial DNA was quantified by quantitative PCR using the following 16S rRNA universal primers: *I6SDPO*-forward 5'-AGAGTTTGATCMTGGCTCA-I-I-I-I-I-AACGCT-3'; *I6SDPO*-reverse 5'-CGCGGCTGCTGGCA-I-I-I-A-I-TTRGC-3' or *EUBAC*-forward, 5'-TCCTACGGGAGGCAGCAGT-3'; *EUBAC*-reverse, 5'-GGACTACCAGGGTATCTAATCCTGTT-3' as previously reported.^{76,77} Quantitative PCR for total bacteria were carried out using a SYBR Premix EX Taq™ and ABI PRISM 7300 quantitative PCR System (Applied Biosystems, Waltham, MA, USA).

Statistical analysis

All values were expressed as means \pm SD. A two-tailed Student *t* test was employed to compare the values between groups. Survival of mice after colitis induction was plotted according to the Kaplan-Meier method and compared using the log-rank test. *P* values less than 0.05 were considered significant.

Abbreviations

Ab	antibody
ADGRE1	adhesion G protein-coupled receptor E1
ATG7	autophagy related 7
AUC	area under the curve
CASP1	caspase 1
CCL2	chemokine (C-C motif) ligand 2
CFSE	carboxyfluorescein succinimidyl ester
CLS	crown-like structure
CXCL1	chemokine (C-X-C motif) ligand 1
DSS	dextran sodium sulfate
ER	endoplasmic reticulum
FOXP3	forkhead box P3
IBD	inflammatory bowel disease
IL1B	interleukin 1 beta
IL6	interleukin 6
IL17A	interleukin 17A
IL2RA	interleukin 2 receptor, alpha chain
IFNG	interferon gamma
IPGTT	intraperitoneal glucose tolerance test
ITGAM	integrin alpha M
ITT	insulin tolerance test
MAP1LC3A/B	microtubule-associated protein 1 light chain 3, alpha/beta
LPS	lipopolysaccharide
M ϕ	macrophage
NAD	nicotinamide adenine dinucleotide
NLRP3	NLR family, pyrin domain containing 3
PA	palmitic acid
ROS	reactive oxygen species
SVF	stromal vascular fraction
T2D	type 2 diabetes
Th	T helper
TLR	toll-like receptor
TGFB	transforming growth factor, beta
TNF	tumor necrosis factor
Treg	regulatory T

Disclosure of potential conflicts of interest

No potential conflicts of interest were disclosed.

Funding

This study was supported by the Global Research Laboratory Grant of the National Research Foundation of Korea (NRF-2010-00347) and the Samsung Biomedical Research Institute grant (C-B1-120). M-SL is the recipient of the Ulsan National Institute of Science and Technology Research Fund (2014M3A9D8034459) and the Bio & Medical Technology Development Program Fund of the National Research Foundation (NRF-2015M3A9B6073846).

References

- [1] Mizushima N, Komatsu M. Autophagy: renovation of cells and tissues. *Cell* 2011; 147:728-41; PMID:22078875; <http://dx.doi.org/10.1016/j.cell.2011.10.026>
- [2] Ozcan U, Cao Q, Yilmaz E, Lee A-H, Iwakoshi NN, Ozdelen E, Tuncman G, Gorgun C, Glimcher LH, Hotamisligil GS. Endoplasmic reticulum stress links obesity, insulin action, and type 2 Diabetes.

- Science 2004; 306:457-61; PMID:15486293; <http://dx.doi.org/10.1126/science.1103160>
- [3] Petersen KF, Befroy D, Dufour S, Dziura J, Ariyan C, Rothman DL, DiPietro L, Cline GW, Shulman GI. Mitochondrial dysfunction in the elderly: possible role in insulin resistance. *Science* 2003; 300:1140-2; PMID:12750520; <http://dx.doi.org/10.1126/science.1082889>
- [4] Quan W, Hur KY, Lim Y, Oh SH, Lee J-C, Kim HC, Kim G-H, Kim S-H, Kim HL, Lee M-K, et al. Autophagy deficiency in beta cells leads to compromised unfolded protein response and progression from obesity to diabetes in mice. *Diabetologia* 2012; 55:392-403; PMID:22075916; <http://dx.doi.org/10.1007/s00125-011-2350-y>
- [5] Kim KH, Lee M-S. Autophagy-a key player in cellular and body metabolism. *Nat Rev Endocrinol* 2014; 10:322-37; PMID:24663220; <http://dx.doi.org/10.1038/nrendo.2014.35>
- [6] Lim Y-M, Lim H-J, Hur KY, Quan W, Lee H-Y, Cheon H, Ryu D, Koo SH, Kim HL, Kim J, et al. Systemic autophagy insufficiency compromises adaptation to metabolic stress and facilitates progression from obesity to diabetes. *Nat Commun* 2014; 5:4934; PMID:25255859; <http://dx.doi.org/10.1038/ncomms5934>
- [7] Johnson AMF, Olefsky JM. The origins and drivers of insulin resistance. *Cell* 2013; 152:673-84; PMID:23415219; <http://dx.doi.org/10.1016/j.cell.2013.01.041>
- [8] Stienstra R, van Diepen JA, Tack CJ, Zaki MH, van de Veerdonk FL, Perera D, Neale GA, Hooiveld GJ, Hijmans A, Vroegrijk I, et al. Inflammasome is a central player in the induction of obesity and insulin resistance. *Proc Natl Acad Sci USA* 2011; 108:15324-9; PMID:21876127; <http://dx.doi.org/10.1073/pnas.1100255108>
- [9] Vandanmagsar B, Youm Y-H, Ravussin A, Galgani JE, Stadler K, Mynatt RL, Ravussin E, Stephens JM, Dixit WD. The NLRP3 inflammasome instigate obesity-induced inflammation and insulin resistance. *Nat Med* 2011; 15:179-88; PMID:21217695; <http://dx.doi.org/10.1038/nm.2279>
- [10] Wen H, Gris D, Lei Y, Jha S, Zhang L, Huang MT, Brickey WJ, Ting JP. Fatty acid-induced NLRP3-ASC inflammasome activation interferes with insulin signaling. *Nat Immunol* 2011; 12:408-15; PMID:21478880; <http://dx.doi.org/10.1038/ni.2022>
- [11] Shi CS, Shenderov K, Huang NN, Kabat J, Abu-Asab M, Fitzgerald KA, Sher A, Kehrl JH. Activation of autophagy by inflammatory signals limits IL-1 β production by targeting ubiquitinated inflammasomes for destruction. *Nat Immunol* 2012; 13:255-63; PMID:22286270; <http://dx.doi.org/10.1038/ni.2215>
- [12] Zhou R, Yazdi AS, Menu P, Tshopp J. A role for mitochondria in NLRP3 inflammasome activation. *Nature* 2011; 469:221-6; PMID:21124315; <http://dx.doi.org/10.1038/nature09663>
- [13] Ebato C, Uchida T, Arakawa M, Komatsu M, Ueno T, Komiya K, Azuma K, Hirose T, Tanaka K, Kominami E, et al. Autophagy is important in islet homeostasis and compensatory increase of beta cell mass in response to high-fat diet. *Cell Metab* 2008; 8:325-32; PMID:18840363; <http://dx.doi.org/10.1016/j.cmet.2008.08.009>
- [14] Jung HS, Chung KW, Kim JW, Kim J, Komatsu M, Tanaka K, Nguyen YH, Kang TM, Yoon KH, Kim JW, et al. Loss of autophagy diminishes pancreatic β -cell mass and function with resultant hyperglycemia. *Cell Metab* 2008; 8:318-24; PMID:18840362; <http://dx.doi.org/10.1016/j.cmet.2008.08.013>
- [15] Kaushik S, Rodriguez-Navarro JA, Arias E, Kiffin R, Sahu S, Schwartz GJ, Cuervo AM, Singh R. Autophagy in hypothalamic AgRP neurons regulates food intake and energy balance. *Cell Metab* 2011; 14:173-83; PMID:21803288; <http://dx.doi.org/10.1016/j.cmet.2011.06.008>
- [16] Kim KH, Jeong YT, Oh H, Kim S-H, Cho JM, Kim Y-N, Kim SS, Kim DH, Hur KY, Kim HK, et al. Autophagy deficiency leads to protection from obesity and insulin resistance by inducing FGF21 as a 'mitokine'. *Nat Med* 2013; 19:83-92; PMID:23202295; <http://dx.doi.org/10.1038/nm.3014>
- [17] Quan W, Kim H-K, Moon E-Y, Kim SS, Choi CS, Komatsu M, Jeong YT, Lee M-K, Kim K-W, Kim M-S, et al. Role of hypothalamic pro-opiomelanocortin neuron autophagy in the control of appetite and leptin response. *Endocrinology* 2012; 153:1817-26; PMID:22334718; <http://dx.doi.org/10.1210/en.2011-1882>
- [18] Singh R, Kaushik S, Wang Y, Xiang Y, Novak I, Komatsu M, Tanaka K, Cuervo AM, Czaja MJ. Autophagy regulates lipid metabolism. *Nature* 2009; 458:1131-5; PMID:19339967; <http://dx.doi.org/10.1038/nature07976>
- [19] Singh R, Xiang Y, Wang Y, Baikati K, Cuervo AM, Luu YK, Tang Y, Pessin JE, Schwartz GJ, Czaja MJ. Autophagy regulates adipose mass and differentiation in mice. *J Clin Invest* 2009; 119:3329-39; PMID:19855132; <http://dx.doi.org/10.1172/JCI35541>
- [20] Yang L, Li P, Fu S, Calay ES, Hotamisligil GS. Defective hepatic autophagy in obesity promotes ER stress and causes insulin resistance. *Cell Metab* 2010; 11:467-78; PMID:20519119; <http://dx.doi.org/10.1016/j.cmet.2010.04.005>
- [21] Zhang Y, Goldman S, Baerga R, Zhao Y, Komatsu M, Jin S. Adipose-specific deletion of autophagy-related gene 7 (atg7) in mice reveals a role in adipogenesis. *Proc Natl Acad Sci USA* 2009; 106:19860-5
- [22] Massey DCO, Parkes M. Genome-wide association scanning highlights two autophagy genes, ATG16L1 and IRGM, as being significantly associated with Crohn's disease. *Autophagy* 2007; 3:649-51; PMID:17921695; <http://dx.doi.org/10.4161/auto.5075>
- [23] Molodecky NA, Kaplan GG. Environmental risk factors for inflammatory bowel disease. *Gastroenterol Hepatol* 2010; 6:339-46
- [24] Misawa T, Takahama M, Kozaki T, Lee H, Zou J, Saitoh T, Akira S. Microtubule-driven spatial arrangement of mitochondria promotes activation of the NLRP3 inflammasome. *Nat Immunol* 2013; 14:454-60; PMID:23502856; <http://dx.doi.org/10.1038/ni.2550>
- [25] Kim KH, Jeong YT, Kim SH, Lee H-Y, Jung HS, Park KS, Lee M-S. Metformin-induced inhibition of the mitochondrial respiratory chain increases FGF21 expression via ATF4 activation. *Biochem Biophys Res Com* 2013; 440:76-81; PMID:24041694; <http://dx.doi.org/10.1016/j.bbrc.2013.09.026>
- [26] Schroder K, Tschopp J. The inflammasomes. *Cell* 2010; 140:821-32; PMID:20303873; <http://dx.doi.org/10.1016/j.cell.2010.01.040>
- [27] Strissel KJ, Stancheva Z, Miyoshi H, Perfield II JW, DeFuria J, Jick Z, Greenberg AS, Obin MS. Adipocyte death, adipose tissue remodeling, and obesity complications. *Diabetes* 2010; 56:2910-8; PMID:17848624; <http://dx.doi.org/10.2337/db07-0767>
- [28] Youm Y-H, Adijiang A, Vandanmagsar B, Burk D, Ravussin A, Dixit VM. Elimination of the NLRP3-ASC inflammasome protects against chronic obesity-induced pancreatic damage. *Endocrinology* 2012; 152:4039-45; PMID: 21862613; <http://dx.doi.org/10.1210/en.2011-1326>
- [29] Feuerer M, Herrero L, Cipolletta D, Naaz A, Wong J, Nayer A, Lee J, Goldfine AB, Benoist C, Shoelson S, et al. Lean, but not obese, fat is enriched for a unique population of regulatory T cells that affect metabolic parameters. *Nat Med* 2009; 15:930-9; PMID:19633656; <http://dx.doi.org/10.1038/nm.2002>
- [30] O'Sullivan BJ, Thomas HE, Pai S, Santamaria P, Iwakura Y, Steptoe R, Kay TWH, Thomas R. IL-1 β breaks tolerance through expansion of CD25⁺ effector T cells. *J Immunol* 2006; 176:7278-87; PMID:16751371; <http://dx.doi.org/10.4049/jimmunol.176.12.7278>
- [31] Yang XO, Nurieva R, Martinez GJ, Kang HS, Chung Y, Pappu BP, Shah B, Chang SH, Schluns KS, Watowich SS, et al. Molecular antagonism and plasticity of regulatory and inflammatory T cell programs. *Immunity* 2008; 29:44-56; PMID:18585065; <http://dx.doi.org/10.1016/j.immuni.2008.05.007>
- [32] Tang Q, Adams JY, Penaranda C, Melli K, Piaggio E, Sgouroudis E, Piccirillo CA, Salomon BL, Bluestone JA. Central role of defective interleukin-2 production in the triggering of islet autoimmune destruction. *Immunity* 2008; 28:687-97; PMID:18468463; <http://dx.doi.org/10.1016/j.immuni.2008.03.016>
- [33] Farache J, Zigmund E, Shakhar G, Jung S. Contributions of dendritic cells and macrophages to intestinal homeostasis and immune defense. *Immunol Cell Biol* 2013; 91:232-9; PMID:23399695; <http://dx.doi.org/10.1038/icc.2012.79>
- [34] Zaki MH, Boyd K, Vogel P, Kastan MB, Lamkanfi M, Kanneganti TD. The NLRP3 inflammatome protects against loss of epithelial integrity and mortality during experimental colitis. *Immunity* 2010; 32:379-91; PMID:20303296; <http://dx.doi.org/10.1016/j.immuni.2010.03.003>

- [35] Bauer C, Diewell P, Mayer C, Lehr HA, Fitzgerald KA, Dauer M, Tschopp J, Endres S, Latz E, Schnurr M. Colitis induced in mice with dextran sulfate sodium (DSS) is mediated by the NLRP3 inflammasome. *Gut* 2010; 59:1192-9; PMID:20442201; <http://dx.doi.org/10.1136/gut.2009.197822>
- [36] Saitoh T, Fujita N, Jang MH, Uematsu S, Yang BG, Satoh T, Omori H, Noda T, Yamamoto N, Komatsu M, et al. Loss of the autophagy protein Atg16L1 enhances endotoxin-induced IL-1 β production. *Nature* 2008; 456:264-9; PMID:18849965; <http://dx.doi.org/10.1038/nature07383>
- [37] Siegmund B, Lehr HA, Fantuzzi G, Dinarello CA. IL-1 β -converting enzyme (caspase-1) in intestinal inflammation. *Proc Natl Acad Sci USA* 2001; 98:13249-54; PMID:11606779; <http://dx.doi.org/10.1073/pnas.231473998>
- [38] Yamamoto M, Yoshizaki K, Kishimoto T, Itoh H. IL-6 is required for the development of Th1 cell-mediated murine colitis. *J Immunol* 2000; 164:4878-82; PMID:10779797; <http://dx.doi.org/10.4049/jimmunol.164.9.4878>
- [39] Khan WI, Motomura Y, Wang H, El-Sharkawy RTE, Verdu EF, Verma-Gandhu M, Rollins BJ, Collins SM. Critical role of MCP-1 in the pathogenesis of experimental colitis in the context of immune and enterochromaffin cells. *Am J Physiol* 2006; 291:G803-11; PMID:16728728; <http://dx.doi.org/10.1152/ajpcell.00457.2005>
- [40] Kim YG, Kamada N, Shaw MW, Warner N, Chen GY, Franchi L, Nunez G. The NOD2 sensor promotes intestinal pathogen eradication via the chemokine CCL2-dependent recruitment of inflammatory monocytes. *Immunity* 2011; 34:769-80; PMID:21565531; <http://dx.doi.org/10.1016/j.immuni.2011.04.013>
- [41] Ranganathan P, Jayakumar C, Manicassamy S, Ramesh G. CXCR2 knock-out mice are protected against DSS-colitis-induced acute kidney injury and inflammation. *Am J Physiol* 2013; 305:F1422-7
- [42] Alex P, Zachos NC, Nguyen T, Gonzales L, Chen T-E, Conklin LS, Cantola M, Li X. Distinct cytokine patterns identified from multiplex profiles of murine DSS and TNBS-induced colitis. *Inflamm Bowel Dis* 2009; 15:341-52; PMID:18942757; <http://dx.doi.org/10.1002/ibd.20753>
- [43] Fuss IJ, Becker C, Yang Z, Groden C, Hurnung RL, Heller F, Neurath MF, Strober W, Mannon PJ. Both IL-12p70 and IL-23 are synthesized during active Crohn's disease and are down-regulated by treatment with anti-IL-12 p40 monoclonal antibody. *Inflamm Bowel Dis* 2006; 12:9-15; PMID:16374252; <http://dx.doi.org/10.1097/01.MIB.0000194183.92671.b6>
- [44] Kimura A, Kishimoto T. Th17 cells in inflammation. *Int Immunopharmacol* 2011; 11:319-22; PMID:21035432; <http://dx.doi.org/10.1016/j.intimp.2010.10.004>
- [45] Yang CS, Kim JJ, Lee HM, Jin HS, Lee SH, Park JH, Kim SJ, Kim JM, Han YM, Lee MS, et al. The AMPK-PPARGC1A pathway is required for antimicrobial host defense through activation of autophagy. *Autophagy* 2014; 10:in press
- [46] Zhao Z, Fux B, Goodwin M, Dunay IR, Strong D, Miller BC, Cadwell K, Delgado MA, Ponpuak M, Green KG, et al. Autophagosome-independent essential function for the autophagy protein Atg5 in cellular immunity to intracellular pathogens. *Cell Host Microbe* 2008; 4:458-69; PMID:18996346; <http://dx.doi.org/10.1016/j.chom.2008.10.003>
- [47] Liu K, Zhao E, Ilyas G, Lalazar G, Lin Y, Haseeb M, Tanaka KE, Czaja MJ. Impaired macrophage autophagy increases the immune response in obese mice by promoting proinflammatory macrophage polarization. *Autophagy* 2015; 11:271-84; PMID:25650776; <http://dx.doi.org/10.1080/15548627.2015.1009787>
- [48] Luan B, Goodarzi MO, Phillips NG, Guo X, Chen YD, Yao J, Allison M, Rotter JI, Shaw R, Montminy M. Leptin-mediated increases in catecholamine signaling reduce adipose tissue inflammation via activation of macrophage HDAC4. *Cell Metab* 2014; 19:1058-65; PMID:24768298; <http://dx.doi.org/10.1016/j.cmet.2014.03.024>
- [49] Clausen BE, Burkhardt C, Reith W, Renkawitz R, Förster I. Conditional gene targeting in macrophages and granulocytes using LysM-cre mice. *Transgenic Res* 1999; 8:265-77; PMID:10621974; <http://dx.doi.org/10.1023/A:1008942828960>
- [50] Talukdar S, Oh DY, Bandyopadhyay G, Li D, Xu J, McNelis J, Lu M, Li P, Yan Q, Zhu Y, et al. Neutrophils mediate insulin resistance in mice fed a high-fat diet through secreted elastase. *Nat Med* 2012; 18:1407-12; PMID:22863787; <http://dx.doi.org/10.1038/nm.2885>
- [51] Yekollu SK, Thomas R, O'Sullivan B. Targeting curcumin to inflammatory dendritic cells inhibits NF- κ B and improves insulin resistance in obese mice. *Diabetes* 2011; 60:2928-38; PMID:21885868; <http://dx.doi.org/10.2337/db11-0275>
- [52] Razani B, Feng C, Coleman T, Emanuel R, Wen H, Hwang S, Ting JP, Virgin HW, Kastan MB, Semenkovich CF. Autophagy links inflammasomes to atherosclerotic progression. *Cell Metab* 2012; 15:533-44; PMID:22440612; <http://dx.doi.org/10.1016/j.cmet.2012.02.011>
- [53] Cani PD, Amar J, Iglesias MA, Poggi M, Knauf C, Bastelica D, Neyrinck AM, Fava F, Tuohy KM, Chabo C, et al. Metabolic endotoxemia initiates obesity and insulin resistance. *Diabetes* 2007; 56:1761-72; PMID:17456850; <http://dx.doi.org/10.2337/db06-1491>
- [54] Shin N-R, Lee J-C, Lee Y-Y, Kim M-S, Whon TW, Lee M-S, Bae J-W. An increase in the Akkermansia sp. population induced by metformin treatment improves glucose homeostasis in diet-induced obese mice. *Gut* 2014; 63:727-35; PMID:23804561; <http://dx.doi.org/10.1136/gutjnl-2012-303839>
- [55] Pal D, Dasgupta S, Kundu R, Maitra S, Das G, Mukhopadhyay S, Ray S, Majumdar SS, Bhattacharya S. Fetuin-A acts as an endogenous ligand of TLR4 to promote lipid-induced insulin resistance. *Nat Med* 2012; 18:1279-85; PMID:22842477; <http://dx.doi.org/10.1038/nm.2851>
- [56] Netea MG, Joosten LA, Lewis E, Jensen DR, Voshol PJ, Kullberg B, Tack CJ, van Krieken H, Kim SH, Stalenhoef AF, et al. Deficiency of interleukin-18 in mice leads to hyperphagia, obesity and insulin resistance. *Nat Med* 2006; 12:650-6; PMID:16732281; <http://dx.doi.org/10.1038/nm1415>
- [57] Cayrol C, Girard JP. The IL-1-like cytokine IL-33 is inactivated after maturation by caspase-1. *Proc Natl Acad Sci USA* 2009; 106:9021-6; PMID:19439663; <http://dx.doi.org/10.1073/pnas.0812690106>
- [58] Bapat SP, Suh JM, Fang SM, Liu S, Zhang Y, Cheng A, Zhou C, Liang Y, LeBlanc M, Liddle C, et al. Depletion of fat-resident Treg cells prevents age-associated insulin resistance. *Nature* 2015; 528:137-41; PMID:26580014; <http://dx.doi.org/10.1038/528S137a>
- [59] Larsen CM, Faulenbach M, Vaag A, Volund A, Ehses JA, Seifert B, Mandrup-Poulsen T, Donath MY. Interleukin-1-receptor antagonist in type 2 diabetes mellitus. *New Engl J Med* 2007; 356:1517-26; PMID:17429083; <http://dx.doi.org/10.1056/NEJMoa065213>
- [60] Owyang AM, Maedler K, Gross K, Yin J, Esposito L, Shu L, Jadhav J, Domsen E, Bergmann J, Lee S, et al. XOMA 052, an anti-IL1 β monoclonal antibody, improves glucose control and b-cell function in the diet-induced obesity mouse model. *Endocrinology* 2010; 151:2515-27; PMID:20332197; <http://dx.doi.org/10.1210/en.2009-1124>
- [61] Masters SL, Dunne A, Subramanian SL, Hull RL, Tannahill GM, Sharp FA, Becker C, Franchi L, Yoshihara E, Chen Z, et al. Activation of the NLRP3 inflammasome by islet amyloid polypeptide provides a mechanism for enhanced IL-1 β in type 2 diabetes. *Nat Immunol* 2010; 11:897-904; PMID:20835230; <http://dx.doi.org/10.1038/ni.1935>
- [62] Westermark P, Andersson A, Westermark GT. Islet amyloid polypeptide, islet amyloid, and diabetes mellitus. *Physiol Rev* 2011; 91:795-826; PMID:21742788; <http://dx.doi.org/10.1152/physrev.00042.2009>
- [63] Cabrera S, Fernández AF, Mariño G, Aguirre A, Suárez MF, Español Y, Vega JA, Laurà R, Fueyo A, Fernández-García MS, et al. ATG4B/autophagin-1 regulates intestinal homeostasis and protects mice from experimental colitis. *Autophagy* 2013; 9:1188-200; PMID:23782979; <http://dx.doi.org/10.4161/auto.24797>
- [64] Cadwell K, Patel KK, Maloney NS, Liu TC, Ng AC, Storer CE, Head RD, Xavier R, Stappenbeck TS, Virgin HW. Virus-plus-susceptibility gene interaction determines Crohn's disease gene Atg16L1 phenotypes in intestine. *Cell* 2010; 141:1135-45; PMID:20602997; <http://dx.doi.org/10.1016/j.cell.2010.05.009>
- [65] Nowarski R, Jackson R, Gagliani N, de Zoete MR, Palm NW, Bailis W, Low JS, Harman CCD, Graham M, Elinav E, et al. Epithelial IL-18 equilibrium controls barrier function in colitis. *Cell* 2015; 163:1444-56; PMID:26638073; <http://dx.doi.org/10.1016/j.cell.2015.10.072>

- [66] Chung Y, Chang SH, Martinez GJ, Yang XO, Nurieva R, Kang HS, Ma L, Watowich SS, Jetten AM, Tian Q, et al. Critical regulation of early Th17 cell differentiation by interleukin-1 signaling. *Immunity* 2009; 30:576-87; PMID:19362022; <http://dx.doi.org/10.1016/j.immuni.2009.02.007>
- [67] Brand S. Crohn's disease: Th1, Th17 of both? The change of a paradigm: new immunological and genetic insights implicate Th17 cells in the pathogenesis of Crohn's disease. *Gut* 2011; 58:1152-67; PMID:19592695; <http://dx.doi.org/10.1136/gut.2008.163667>
- [68] Yen D, Cheung J, Scheerens H, Poulet F, McClanahan T, McKenzie B, Kleinschek MA, Owyang A, Mattson J, Blumenschein W, et al. IL-23 is essential for T cell-mediated colitis and promotes inflammation via IL-17 and IL-6. *J Clin Invest* 2006; 116:1310-6; PMID:16670770; <http://dx.doi.org/10.1172/JCI21404>
- [69] Becker C, Dornhoff H, Neufert C, Fantini MC, Wirtz S, Huebner S, Nikolaev A, Lehr HA, Murphy AJ, Valenzuela DM, et al. Cutting edge: IL-23 cross-regulates IL-12 production in T cell-dependent experimental colitis. *J Immunol* 2006; 177:2760-4; PMID:16920909; <http://dx.doi.org/10.4049/jimmunol.177.5.2760>
- [70] Strober W, Fuss IJ. Proinflammatory cytokines in the pathogenesis of inflammatory bowel diseases. *Gastroenterology* 2011; 140:1756-67; PMID:21530742; <http://dx.doi.org/10.1053/j.gastro.2011.02.016>
- [71] Han MS, Chung KW, Cheon HG, Rhee SD, Yoon C-H, M-K. L, Kim K-W, Lee M-S. Imatinib mesylate reduces endoplasmic reticulum stress and induces remission of diabetes in db/db mice. *Diabetes* 2009; 58:329-36; PMID:19171749; <http://dx.doi.org/10.2337/db08-0080>
- [72] Kim HS, Lee M-S. Essential role of STAT1 in caspase-independent cell death of activated macrophages through the p38 mitogen activated protein kinase/STAT1/reactive oxygen species pathway. *Mol Cell Biol* 2005; 25:6821-33; PMID:16024814; <http://dx.doi.org/10.1128/MCB.25.15.6821-6833.2005>
- [73] Kim HS, Han MS, Chung KW, Kim S, Kim E, Kim MJ, Jang E, Lee HA, Youn J, Akira S, et al. Toll-like receptor 2 senses beta-cell death and contributes to the initiation of autoimmune diabetes. *Immunity* 2007; 27:321-33; PMID:17707128; <http://dx.doi.org/10.1016/j.immuni.2007.06.010>
- [74] Cinti S, Mitchell G, Barbatelli G, Murano I, Ceresi E, Faloia E, Wang S, Fortier M, Greenberg AS, Obin MS. Adipocyte death defines macrophage localization and function in adipose tissue of obese mice and humans. *J Lipid Res* 2005; 46:2347-55; PMID:16150820; <http://dx.doi.org/10.1194/jlr.M500294-JLR200>
- [75] Yu Z, Morrison M. Improved extraction of PCR-quality community DNA from digesta and fecal samples. *Biotechniques* 2004; 36:808-12; PMID:15152600
- [76] Amar J, Chabo C, Waget A, Klopp P, Vachoux C, Bermúdez-Humarán LG, Smirnova N, Bergé M, Sulpice T, Lahtinen S, et al. Intestinal mucosal adherence and translocation of commensal bacteria at the early onset of type 2 diabetes: molecular mechanisms and probiotic treatment. *EMBO Mol Med* 2011; 9:559-72; PMID:21735552; <http://dx.doi.org/10.1002/emmm.201100159>
- [77] Kommedal Ø, Simmon K, Karaca D, Langeland N, Wiker HG. Dual priming oligonucleotides for broad-range amplification of the bacterial 16S rRNA gene directly from human clinical specimens. *J Clin Microbiol* 2012; 50:1289-94; PMID:22278843; <http://dx.doi.org/10.1128/JCM.06269-11>